Journal of ELECTRONIC MATERIALS, Vol. 37, No. 8, 2008
DOI: 10.1007/s11664-008-0490-8

Regular Issue Paper

Effect of Zn Addition on Interfacial Reactions Between Sn-4Ag Solder and Ag Substrates

H.F. ZOU[1] and Z.F. ZHANG[1,2]

1.—Shenyang National Laboratory for Materials Science, Institute of Metal Research, Chinese Academy of Sciences, 72 Wenhua Road, Shenyang 110016, People's Republic of China. 2.—e-mail: zhfzhang@imr.ac.cn

In this study, the effect of Zn (Zn = 1 wt.%, 3 wt.%, and 7 wt.%) additions to Sn-4Ag solder reacting with Ag substrates was investigated under solid-state and liquid-state conditions. The composition and microstructure of the intermetallic compounds (IMCs) significantly changed due to the introduction of different Zn contents. In the case of Sn-4Ag solder with 1 wt.% Zn, a continuous Ag-Sn IMC layer formed on the Ag substrates; discontinuous Ag-Zn layers and Sn-rich regions formed on the Ag substrates under liquid-state conditions when the Sn-4Ag solders contained 3 wt.% and 7 wt.% Zn. If 3 wt.% Zn was added to Sn-4Ag solder, the Ag-Sn IMC would be transformed into a Ag-Zn IMC with increasing aging time. Rough interfaces between the IMCs and the Ag substrates were observed in Sn-4Ag-7Zn/Ag joints after reflowing at 260°C for 15 min; however, the interfaces between the IMCs and the Ag substrates became smooth for Sn-4Ag-1Zn/Ag and Sn-4Ag-3Zn/Ag joints. The nonparabolic growth mechanism of IMCs was probed in the Sn-4Ag-3Zn/Ag joints during liquid-state reaction, and can be attributed to the detachment of IMCs. On the other hand, the effect of gravity was also taken into account to explain the formation of IMCs at the three different interfaces (bottom, top, and vertical) during the reflow procedure.

Key words: Sn-Ag-Zn, lead-free solder, gravity, interfaces, intermetallic compounds

INTRODUCTION

Sn-Pb alloys have been used in electronic packaging for many years, however, lead and its alloys will be forbidden in many countries because of their toxicity, especially in electronic packaging.[1] Therefore, it is an urgent task for electronic packaging and other fields to develop new lead-free solders to replace these conventional Sn-Pb solders.

At present, binary alloys, such as Sn-Ag, Sn-Cu and Sn-Bi, are important lead-free solders in electronic packaging.[2] To further optimize the properties of these binary solders, Ag, Bi, Ni, and Cu are often added to these binary alloys.[3–7] Recently, some researchers revealed that the addition of Zn can optimize the properties of solder joints.[8–16] It was found that the presence of Zn in Sn-Ag solder often results in a significant improvement of the mechanical properties.[8] For example, the tensile strength and elongation of Sn-3.3Ag-*x*Zn (wt.%) solder were dramatically improved[16] due to the introduction of Zn into Pb-10wt.%Sn alloy, which improves the high-temperature plasticity and refines the grain size.[17] In addition, a small amount of Zn addition to a Sn-0.7Cu solder can refine the microstructure of the solders and retard the growth of an IMC layer.[18] It was also found that the addition of Zn simultaneously improved the Vickers hardness, yield strength, and the ductility and restrained the formation of large Ag_3Sn plates in a Pb-1.5Sb alloy.[12,16]

On the other hand, Sn-Ag alloy is one of the good candidates to replace Sn-Pb solders because of its

(Received October 26, 2007; accepted May 9, 2008; published online June 12, 2008)

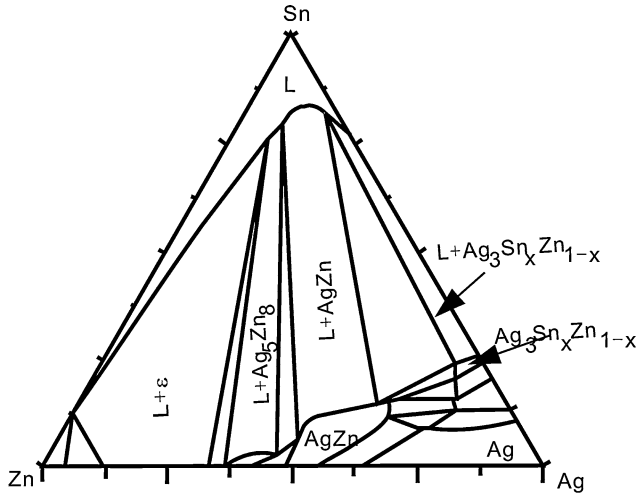

Fig. 1. Isothermal section of Sn-Ag-Zn ternary phase diagram at 380°C.

superior mechanical properties.[16,19,20] As we know, the addition of Zn would improve the mechanical properties, so the ternary Sn-Ag-Zn phase diagram should be considered, as shown in Fig. 1.[21] It is found that Ag-Zn IMCs will replace Ag-Sn IMCs during cooling and Ag-Zn particles tend to sediment in the lower region of the molten solder when using a low cooling rate.[22,23] Song and Lin found that there were two peritectic transformations upon solidification for Sn-9Zn-*x*Ag solders.[22] And it is well known that Ag substrates have many superior properties, such as good conductivity, anti-oxidation, and wettability, which account for Ag substrates wide use in electronic packaging.[24] A considerable number of researchers have focused on the interfacial reactions between Cu or Ni and lead-free solders.[25–29] The effect of Cu addition on the interfacial reactions between Sn-9Zn and Ag substrates has also been investigated.[15] However, there are limited data about the interfacial reactions between Sn-4Ag-*x*Zn and Ag substrates. The main purpose of this study was to investigate the effect of Zn addition on the interfacial reactions between Sn-4Ag solder and Ag substrates.

EXPERIMENTAL PROCEDURE

In this study, Ag single crystals were used as substrates and three Sn-4Ag-*x*Zn alloys (x = 1 wt.%, 3 wt.%, and 7 wt.%) were employed as solders. Firstly, a Ag single-crystal plate with dimensions of 40 mm × 80 mm × 10 mm was grown from Ag with a purity of 99.999% by the Bridgman method in a horizontal furnace. Secondly, the lead-free solders were prepared by melting high-purity (4N) tin, zinc, and silver in vacuum ($<10^{-1}$ Pa) at 800°C for 30 min. The single-crystal Ag and the solders were cut and then ground with 800 grade, 1000 grade, and 2000 grade SiC papers and then carefully polished with 2.5 μm, 1.5 μm, and 0.5 μm polish pastes. They were then ultrasonically cleaned in ethanol for 10 min after polishing. In order to ensure that all the interfacial reactions were conducted under the same conditions, the three solders (about 0.5 g for each solder) were placed on different positions on a single-crystal Ag plate. Finally, the prepared samples were bonded in an oven with a constant temperature of 260°C for 15 min. One group of as-reflowed samples was isothermally aged at 160°C for 0 days, 2 days, 4 days, 7 days, and 11 days in order to study the IMC growth kinetics under the solid-state conditions. Another group of as-reflowed samples was isothermally aged at 260°C for various durations so as to reveal the IMC growth kinetics under liquid-state conditions. After solid- and liquid-state reactions, all the samples were observed with a LEO super35 scanning electron microscope (SEM) to detect the morphologies and thickness of the interfacial IMC layers. In order to decrease the error, both the integral area and the length of the IMC layers were measured using special software (SISC IAS V 8.0). The average thickness of the IMC layers can be calculated by using the following equation

$$d = \int_0^{L_0} f(x)dx/L_0. \quad (1)$$

where L_0 is the length of the measured region, $f(x)$ is the contour function of the IMC, and d is the average thickness of the IMC layer. To reveal the morphologies of the reactive phases between the Ag single crystal and the Sn-4Ag-*x*Zn solders, some samples aged at 260°C for 22 h were deeply etched with 5% HCl + 3% HNO_3 + CH_3OH (vt%) etchant solution to remove the excess Sn phase so that the reactive phases could be well exposed.

EXPERIMENTAL RESULTS

Interfacial Reactions Between Sn-4Ag-1Zn and Ag

Figure 2 shows interfacial morphologies of the couples under solid-state and liquid-state conditions after different periods. Under liquid-state conditions, there is only one IMC layer, which was detected as $Ag_{73}Sn_{25}Zn_2$ (or Ag_3Sn) with energy-dispersive spectroscopy (EDS). Therefore, the reaction product of Sn-4Ag-1Zn and Ag is the same as that of Sn-4Ag and Ag. The reaction product of Sn-0.5Zn and Cu is the same as that of Sn and Cu too.[14] Meanwhile, the interfaces become rougher with increasing aging time, as illustrated in Fig. 2 a–c, which is similar to previous results.[15,27] However, the reaction products of the solid-state reaction are quite different from those of the liquid-state reaction; two IMC layers formed at the interface. One IMC layer is $Ag_{58}Sn_{26}Zn_{16}$, and the second, gray layer (the inner Ag-Zn IMC layer) is $Ag_{72}Zn_{24}Sn_4$ (Ag_3(Zn,Sn)). The thickness of the $Ag_{72}Zn_{24}Sn_4$ (Ag_3(Zn,Sn)) layer remains unchanged with increasing aging time.

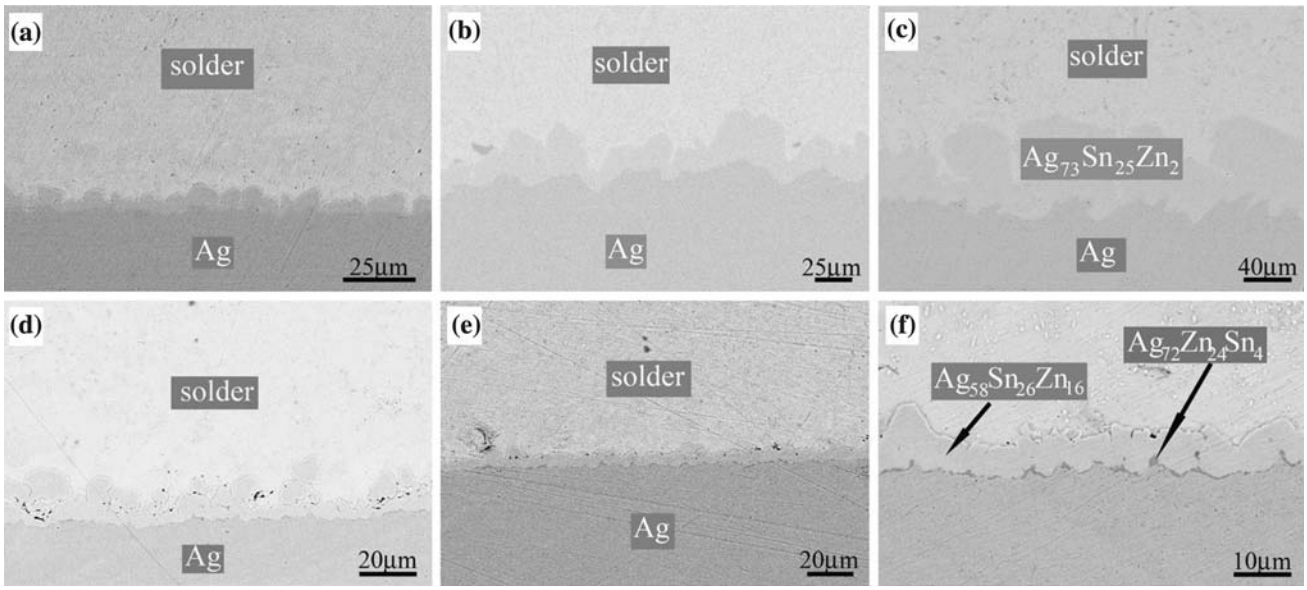

Fig. 2. Interfacial morphologies of the Sn-4Ag-1Zn solder reacted with single-crystal Ag, (a) as-reflowed; and after aging for (b) 8 h and (c) 22 h at 260°C; and (d) 2 days, (e) 7 days, and (f) 11 days at 160°C.

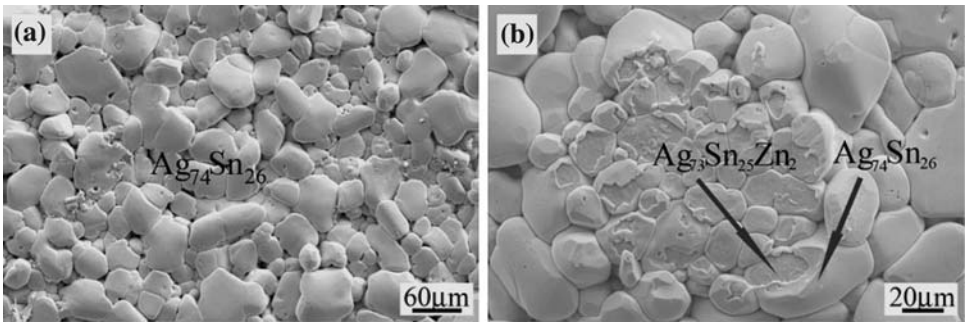

Fig. 3. IMC morphology of the deep-etched Sn-4Ag-1Zn/Ag solder joint after aging at 260°C for 22 h.

Figure 3 shows an IMC micrograph of a deep-etched Sn-4Ag-1Zn/Ag couple aged at 260°C for 22 h. It can be seen that the IMC grains became rather coarse and compact, and two different IMC layers appeared. After analysis with EDS, the outer layer was identified as the $Ag_{74}Sn_{26}$ phase and the inner layer as the $Ag_{73}Sn_{25}Zn_2$ phase. Experimental results indicate that the effect of Zn on the interfacial reaction is not obvious due to its low concentration (1 wt.%) in the solder.

Interfacial Reactions Between Sn-4Ag-3Zn and Ag

Figure 4 shows a backscattering electron image of the interfaces between Sn-4Ag-3Zn and Ag substrates. Only a $Ag_{48}Zn_{48}Sn_4$ (or AgZn) IMC layer was found on the Ag substrates when samples were aged at 260°C for 15 min (as reflowed), as illustrated in Fig. 4a. However, two additional IMC layers were formed at the interface when the samples were aged at 260°C for 8 h, as shown in Fig. 4b. In particular, it is interesting to find that the original $Ag_{48}Zn_{48}Sn_4$ IMC spalled off from the $(Ag,Zn)_3Sn$ IMC layer. Besides, many Sn-rich regions and some $(Ag,Zn)_3Sn$ IMCs began to form above the original $Ag_{48}Zn_{48}Sn_4$ IMC after aging, as displayed in Fig. 4b. With further increasing aging time, the $(Ag,Zn)_3Sn$ IMC had almost replaced the $Ag_{48}Zn_{48}Sn_4$ IMC, and dendritic IMCs were formed near the interface, as indicated in Fig. 4c. In addition, some AgZn IMCs had been transformed into the $(Ag,Zn)_3Sn$ IMC under solid-state conditions, as illustrated in Fig. 4d and e. As a result, two IMC layers were formed at the interface during the solid-state reaction. When aging time increased to 7 days, there is still one thin AgZn IMC layer, which cannot be transformed into Ag-Sn IMC, which may be ascribed to the equilibrium of Zn diffusion. Therefore, the thickness of the inner Ag-Zn-Sn IMC layer is unchanged with increasing aging time, as shown in Fig. 4d–f.

Figure 5 shows the IMC morphologies of a deep-etched Sn-4Ag-3Zn/Ag couple reacted at 260°C for 22 h. Several spherical IMCs with different sizes

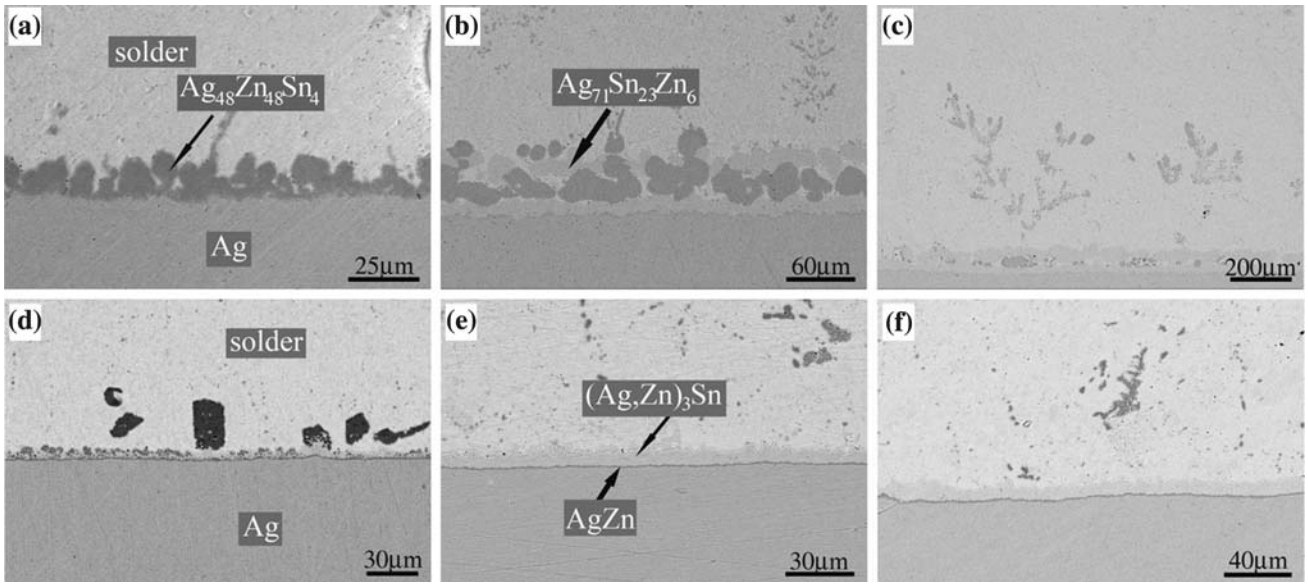

Fig. 4. Interfacial morphologies of Sn-4Ag-3Zn reacted with single-crystal Ag: (a) as-reflowed; after aging for (b) 8 h and (c) 22 h at 260°C; and (d) 2 days, (e) 7 days, and (f) 11 days at 160°C.

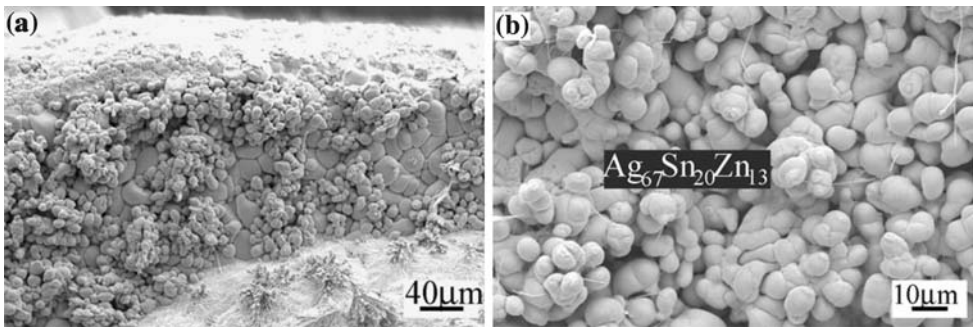

Fig. 5. IMC morphology of the deep-etched Sn-4Ag-3Zn/Ag joint aged at 260°C for 22 h.

are clearly observed in Fig. 5a and b. It is apparent that two kinds of IMCs are formed at the interface. Therefore, it can be concluded that the interface reaction and the IMCs dramatically changed when the concentration of Zn increased to 3 wt.%.

Interfacial Reactions Between Sn-4Ag-7Zn and Ag

A backscattering electron image of the interface between Sn-4Ag-7Zn and the Ag substrate is shown in Fig. 6. One of the interesting findings is that all interfaces became rather rough under solid-state conditions, as shown in Fig. 6d–f. There are three IMC layers, i.e., $Ag_{75}Sn_9Zn_{16}$ ($Ag_3(Sn,Zn)$), Ag_3Sn, and AgZn, at the interfaces of the as-reflowed sample. Generally speaking, the interface between the solder and the IMC, rather than that between the IMC and the substrates, is always rough because it is the foreland of the reaction.[30] However, the opposite result was obtained in our research. Firstly, some Sn-rich regions were found under liquid-state conditions, which is different from the interfacial reactions between most lead-free (e.g., Sn-In) solders and Ag substrates,[24,26,31] as displayed in Fig. 4. However, Sn-rich regions have been reported in other interfacial reactions, e.g., Sn-Zn/Cu, Sn-Zn-Cu/Ag, and Sn-Zn/Ag.[15,32,33] Secondly, the AgZn IMC layer was completely detached from the Ag_3Sn IMC when the samples were aged at 260°C for 15 min (as reflowed). Meanwhile, the Ag_3Sn phase was formed as some loose particles rather than as a continuous layer between the AgZn IMC and the Ag substrates, as illustrated in Fig. 6a. With increasing reflow time, the volume fraction of the Sn-rich regions or the IMC layers decreased, and the Ag_3Sn IMC gradually formed an entirely continuous layer. However, the IMC has been transformed from AgZn into $Ag_{59}Sn_{29}Zn_{12}$ due to the increase in the concentration of Ag and Sn during the reflow procedure. In addition, looser IMCs and more Sn-rich regions formed at the interface, and the shape of the $Ag_{59}Sn_{29}Zn_{12}$ IMC tends to be spherical, as shown in Fig. 6b and c.

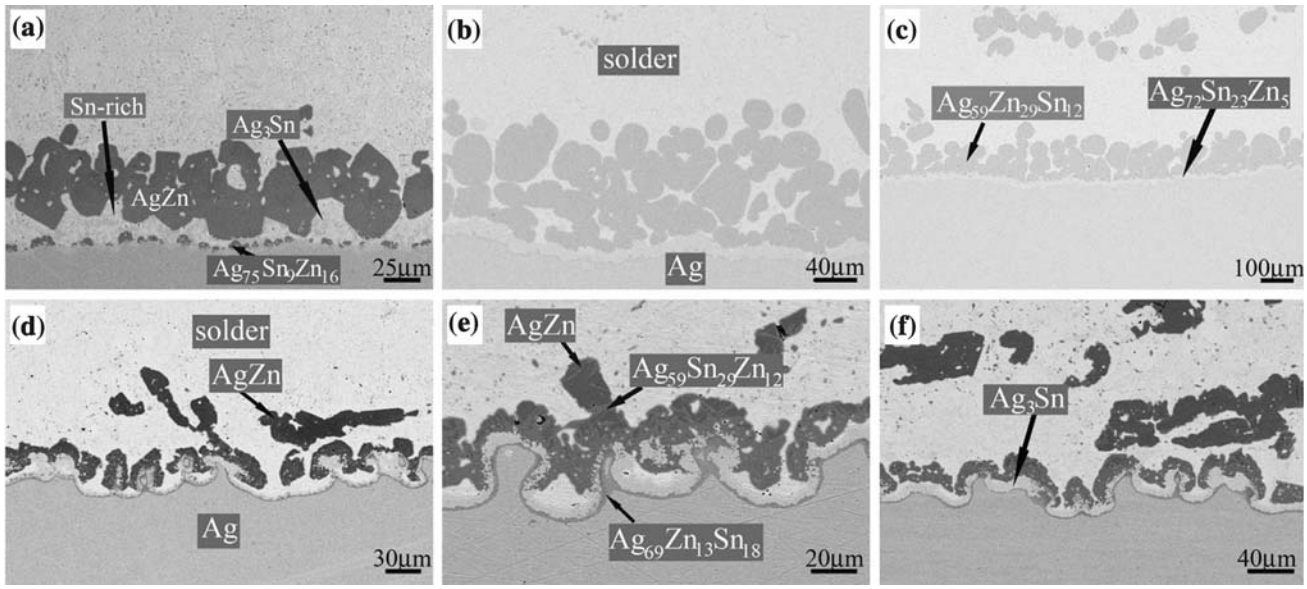

Fig. 6. Interfacial morphologies of the Sn-4Ag-7Zn reacted with single-crystal Ag: (a) as-reflowed; after aging for (b) 8 h and (c) 22 h at 260°C; and (d) 2 days, (e) 7 days, and (f) 11 days at 160°C.

Under solid-state conditions, the composition of the Ag-Zn IMC also changed with increasing aging time, as shown in Fig. 6d–f. Figure 6d shows that the AgZn IMC is dominant after aging at 160°C for 2 days; however, some needle-like $Ag_{59}Sn_{29}Zn_{12}$ IMCs were gradually formed in AgZn with increasing aging time, as displayed in Fig. 6e. The total thickness of the Ag_3Sn and $Ag_{69}Zn_{13}Sn_{18}$ IMCs became thicker. Sn-rich regions were also found in these samples aged at 160°C. With further extended aging time, the Ag_3Sn and $Ag_{69}Zn_{13}Sn_{18}$ IMCs gradually spread over the Sn-rich region because Ag-Zn particles cannot easily move into the solder under solid-state conditions, as illustrated in Fig. 6e and f. However, the thickness of the bottom $Ag_{69}Zn_{13}Sn_{18}$ IMC is unchanged.

To reveal the effect of gravity on the formation of IMCs during liquid-state reaction, one special sample with three different interfaces was designed, as illustrated in Fig. 7. Figures 8–10 show the IMC morphologies observed on the three different positions (bottom, top, and vertical) of the couples

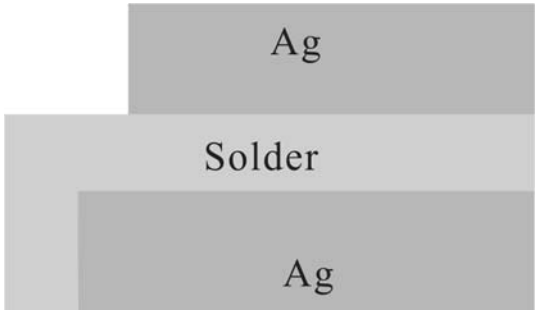

Fig. 7. Schematic diagram of the Sn-4Ag-7Zn/Ag joint reacted at different positions.

reacted at 260°C for different times. Many differences were observed among the three different interfaces. For the as-reflowed sample, besides the lateral interface, some Sn-rich regions and loose Ag_3Sn particles were formed between the Ag-Zn IMC and the Ag substrates, as displayed in Figs. 8a and 9a. However, the composition of the AgZn IMC changed with extended aging time. The AgZn IMC was gradually transformed into the $Ag_{59}Zn_{29}Sn_{12}$ IMC, as indicated by arrows in Figs. 8a, b and 9a, b. A continuous Ag_3Sn IMC layer, rather than a Sn-rich region or loose Ag_3Sn particles, was formed at the lateral interface, as shown in Fig. 10, which is quite different from the top and bottom interfaces.

With increasing aging time, the volume fraction of the Sn-rich region dramatically decreased on the bottom and top interfaces. However, the volume fraction of the Sn-rich region on the bottom interface is still higher than that on the top interface. In comparison with the top and bottom interfaces, it is interesting to find that the constitution of the lateral interface changed from solder/Ag_3Sn/$Ag_{69}Zn_{18}Sn_{13}$/Ag to solder/$Ag_{59}Zn_{29}Sn_{12}$/Ag_3Sn/$Ag_{69}Zn_{18}Sn_{13}$/Ag. With further increasing aging time, the outer $Ag_{59}Zn_{29}Sn_{12}$ IMC layer started to detach from the Ag_3Sn IMC layer, and then many spherical IMC particles were formed, as indicated in Fig. 10b and c. Finally, these spherical $Ag_{59}Zn_{29}Sn_{12}$ IMC particles were completely detached from the Ag_3Sn IMC layer, as shown in Fig. 10d; then some dendrites were formed in the solder and some $Ag_{59}Zn_{29}Sn_{12}$ particles dropped into the bottom of the solder.

Figure 11 shows some particles close to the top interface. Some peritectic transformations were observed in the solder. There is a gray IMC layer

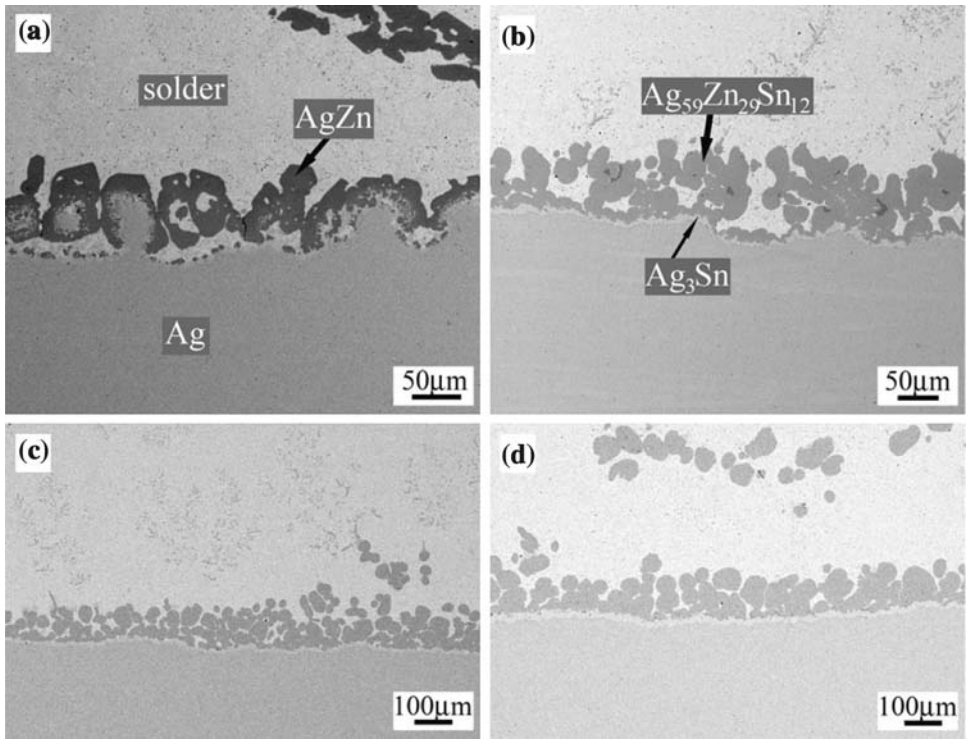

Fig. 8. Microstructure evolution of the bottom IMCs: (a) as-reflowed, and after aging at 260°C for (b) 4 h, (c) 8 h, and (d) 22 h.

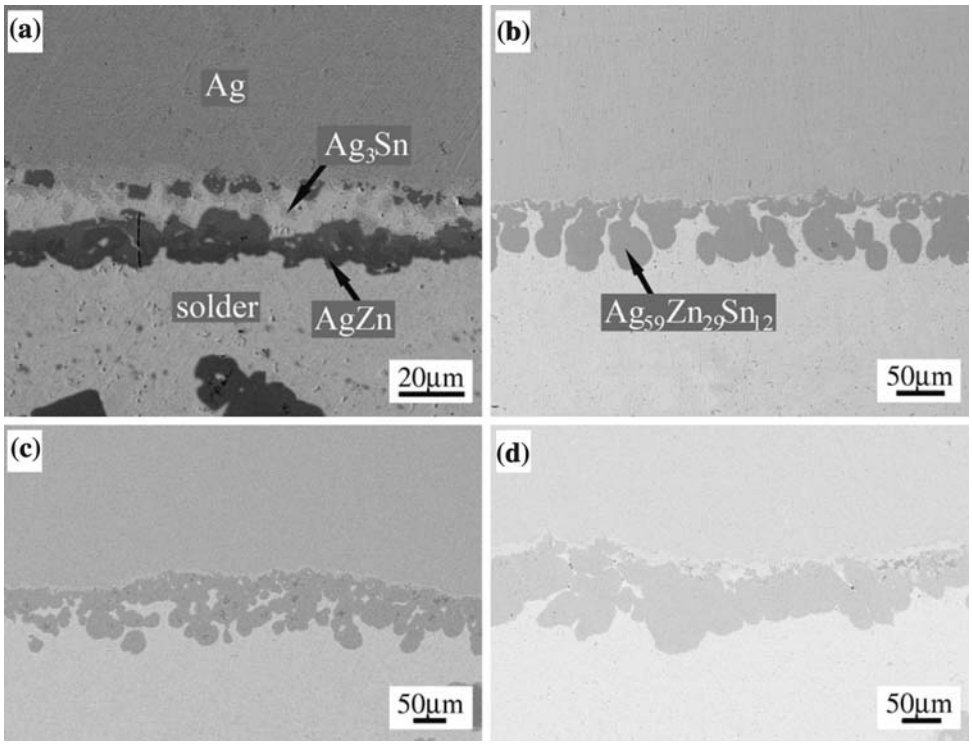

Fig. 9. Microstructure evolution of the top IMCs: (a) as-reflowed, and after aging at 260°C for (b) 4 h, (c) 8 h, and (d) 22 h.

around the black AgZn IMC. Song and Lin[22] reported that there were two peritectic transformations for Sn-9Zn-*x*Ag solder during solidification. In addition to the observations in Fig. 11, the peritectic transformations occurred widely in the top and bottom interfaces, as shown in Figs. 8b and 9b, c.

Figure 12 shows the IMC morphologies on the bottom and top interfaces for the couple reacted at

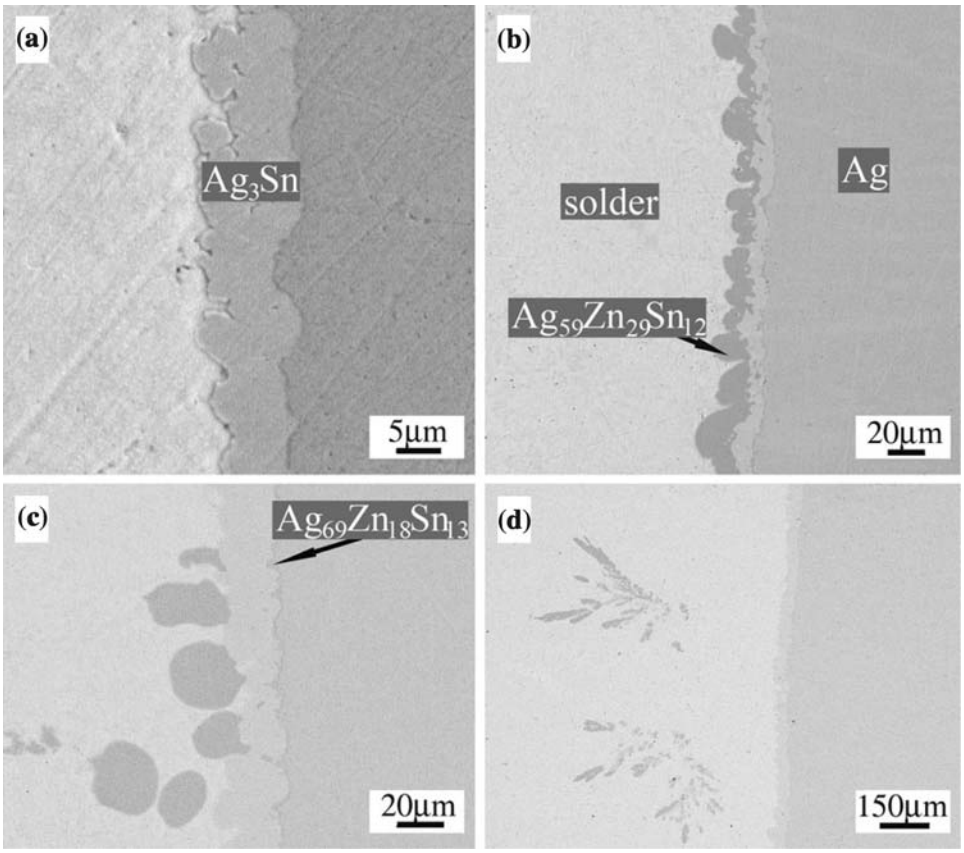

Fig. 10. Microstructure evolution of the lateral IMCs: (a) as-reflowed, and after aging at 260°C for (b) 4 h, (c) 8 h, and (d) 22 h.

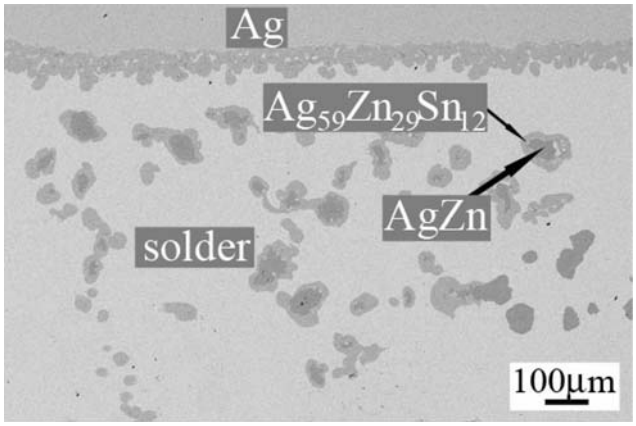

Fig. 11. The peritectic transformations of the Sn-4Ag-7Zn and Ag substrate.

260°C for 22 h after deep etching. It is interesting to note that there are still two different microstructures of Ag-Zn-Sn IMCs. On the bottom interface, there are many spherical particles, as indicated in Fig. 12a and b; however, on the top interface, some polyhedral (hexagonal) particles were observed, as denoted in Fig. 12c and d. Muldawer[34] found that slow cooling or continuous heating at temperatures above 100°C gave rise to the AgZn phase with a complex hexagonal structure. In addition to the spherical or polyhedral (hexagonal) particles, many fibers were observed on the bottom interface after deep etching. However the fibers are too thin to identify the composition. Besides, some superlarge IMCs ($Ag_{56}Zn_{33}Sn_{11}$) were also observed in the two interfaces. Polyhedral (hexagonal) particles were not observed at the interface between Sn-4Ag-3Zn and Ag substrates, as indicated in Fig. 5.

DISCUSSION

Interfacial Reaction Product and Detachment of the Ag-Zn IMC

For Sn-4Ag-xZn/Ag (x = 3 wt.% and 7 wt.%) couples, AgZn instead of Ag_3Sn IMC was formed at the interface, which is similar to the interfacial reaction between Sn-Zn-based solders and Ag substrates.[15,32] The interfacial reactions can be described as:

$$3Ag_{(l)} + Sn_{(l)} \rightarrow Ag_3Sn_{(s)}, \quad (2)$$

$$(1-x)Ag + xZn = Ag_{1-x}Zn_x. \quad (3)$$

According to the isothermal equation of chemical reaction, one obtains:

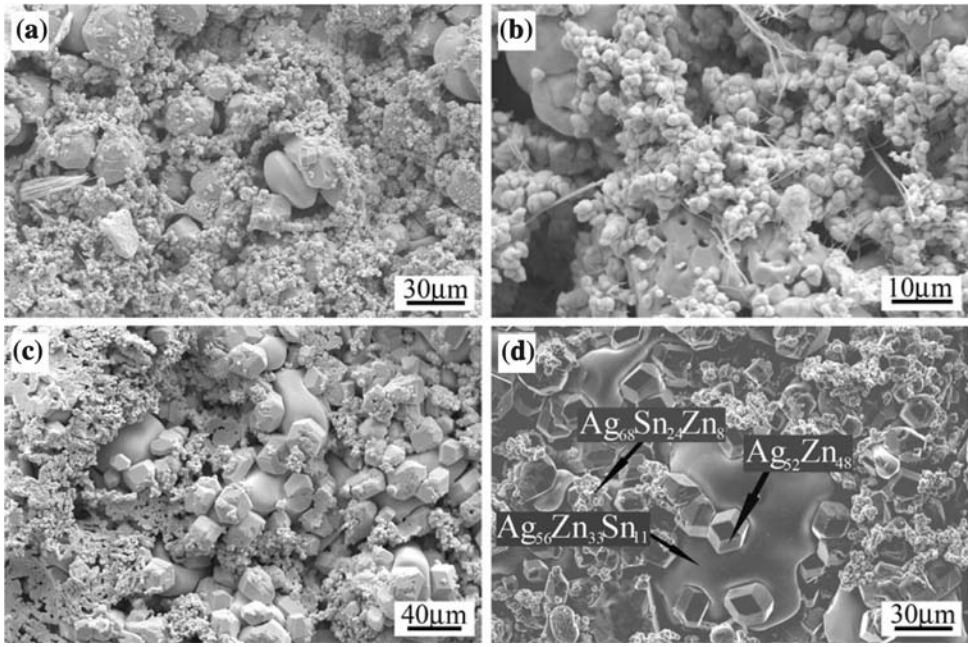

Fig. 12. Interfacial IMC morphologies of the deep-etched Sn-4Ag-7Zn/Ag joint after aging at 260°C for 22 h observed on (a) and (b) bottom interface; (c) and (d) top interface.

$$\Delta G_{Ag_3Sn} = \Delta G_f + RT\mathrm{Ln}\frac{1}{[Sn][Ag]^3} \quad (4)$$

$$\Delta G_{Ag_{1-x}Zn_x} = \Delta G_f + RT\mathrm{Ln}\frac{1}{[Zn]^x[Ag]^{1-x}}, \quad (5)$$

where ΔG and ΔG_f are the Gibbs function of molar reaction and the standard Gibbs function of molar reaction, R is the gas constant, T is the absolute temperature, [Sn], [Ag], and [Zn] are the concentrations of Sn, Ag, and Zn atoms, respectively. From the equations above, it is known that ΔG_f, [Sn], [Zn], and [Ag] play important roles in the formation of IMCs. Table I lists the ΔG_f values of all the Ag-Zn IMCs and the Ag-Sn IMC[35]; it can be found that the ΔG_f values of the Ag-Zn phases are much lower than that of the Ag_3Sn phase, indicating that the Ag-Zn IMC is easier to form during the interfacial reaction. This can explain why Ag-Zn IMCs were often observed in most samples when a small amount of Zn was added into the solder. However, the Sn-4Ag-1Zn couple only formed one thin layer of Ag-Zn IMC under solid-state conditions due to the low concentration of Zn.

The interfacial reactions between Ag and Sn-4Ag-x Zn solders are very sensitive to the Zn concentration. Some Sn-rich regions were formed at the interface between the Ag substrates and the solders except for the Sn-4Ag-1Zn/Ag couple. In addition, the Ag-Zn IMCs were detached from the interface after the reflow procedure, which is similar to many previous results.[36–38] After careful observations, it can be found that the Ag-Zn-Sn IMCs tended to detach from the Ag_3Sn IMC once the Ag_3Sn IMC was formed at the interfaces (Sn-4Ag-3Zn/Ag or Sn-4Ag-7Zn/Ag). Obviously, there is only one interface (Ag-Zn-Sn/Ag_3Sn) before the detachment, but the original interface will be replaced by two new interfaces (Ag-Zn-Sn/solder and Ag_3Sn/solder) after detachment. According to the minimum interfacial energy concept, the inequality $\gamma_{AgZnSn/AgSn} > \gamma_{AgZnSn/solder} + \gamma_{AgSn/solder}$ should be fulfilled.[36] Therefore, the interfacial free energy (γ) results in this detachment, which means weak adhesion between the Ag-Zn-Sn IMCs and the Ag_3Sn IMC (the correlation between the interfacial free energy and the adhesion can be see in Ref. 36).

Growth Kinetics of IMCs

According to the above observations, the thickness of the IMC layers continues to increase. However, the interface between the Sn-4Ag-7Zn solder and the Ag substrates is too rough to measure

Table I. The Standard Gibbs Function of Molar Reaction of $Ag_{1-x}Zn_x$ and Ag_3Sn

X_{Zn}	0.2	0.3	0.348	0.4	0.5	0.558	0.598	0.64	0.678	0.7	0.758	Ag_3Sn (650 K)
ΔG (cal/g-atom)	–1536	–2025	–2181	–2319	–2483	–2475	–2441	–2371	–2275	–2213	–1979	–850

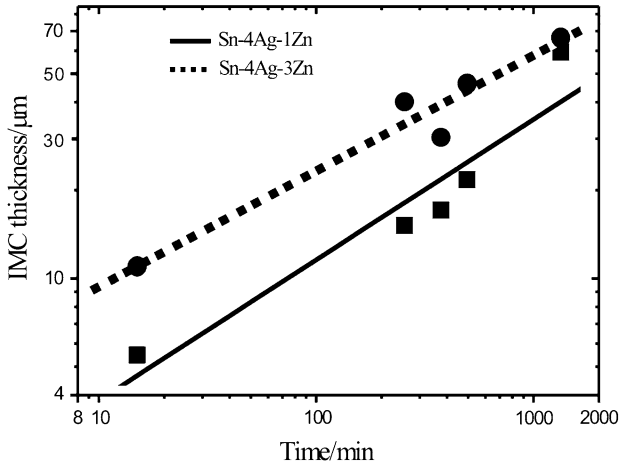

Fig. 13. The growth kinetics of the Sn-4Ag-1Zn/Ag and Sn-4Ag-3Zn/Ag joints aging at 260°C.

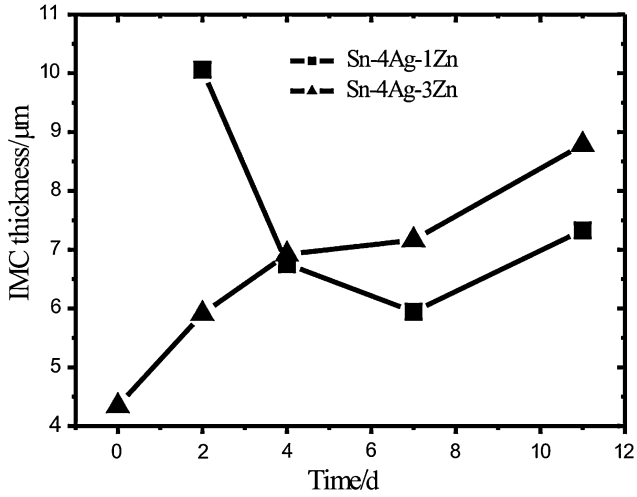

Fig. 14. The growth kinetics of the Sn-4Ag-1Zn/Ag and Sn-4Ag-3Zn/Ag joints aging at 160°C.

the thickness of the IMCs. We only measured and calculated the total thickness of the IMCs between Ag and different solders (Sn-4Ag-1Zn and Sn-4Ag-3Zn) by using Eq. 1. It is found that the thickness of the IMC layers (d) fitted well with the following equation: $d = k \times t^n$, where k, n, and t are two constants and the aging time, respectively. Figure 13 shows the plot of $\lg(d) - \lg(t)$ for the couples reacted under liquid-state conditions. For the Sn-4Ag-1Zn and Sn-4Ag-3Zn solders, the constant n is equal to 0.479 and 0.394, respectively. For Sn-4Ag-3Zn, the IMC growth mechanism is nonparabolic. This phenomena may be attributed to two reasons, one is that some IMCs were detached from the bottom IMC; another is that the limited amount of Zn in the solder inhibited the growth rate of IMCs. As shown in Fig. 11, for example, the thickness of IMCs aged for 375 min is about 30 μm, which is thinner than that (40 μm) after aging for 255 min. A similar nonparabolic mechanism for the growth of IMCs has been probed in many interfacial reactions of soldering joints.[33,39,40] Figure 14 illustrates the relationship between the thickness of the IMCs and the aging time for the two couples aged at 160°C. For the Sn-4Ag-1Zn/Ag couples, the IMCs become thinner at the beginning of the interfacial reaction. In other studies, it has been reported that Zn addition to a Sn-based solder alloy inhibited the growth of IMCs with Cu substrates during isothermal aging.[8,13] After aging for 7 days, the thickness of the IMCs starts to increase. It may be supposed that the IMC growth consists of two different processes, i.e., detachment and growth. When detachment plays a dominant role in the growth of IMCs, the IMC thickness decreases with increasing aging time; in contrast, the IMC thickness increases with increasing aging time. However, for the Sn-4Ag-3Zn couple, the IMC growth mechanism is approximately parabolic, which is similar to most interfacial reactions.[41,42]

For the Sn-4Ag-3Zn and Sn-4Ag-7Zn solders, Ag-Zn IMCs were often formed at the interface in the initial stage during the reflow procedure. However, with extended aging time, the Ag-Zn IMC was transformed into $Ag_{59}Zn_{29}Sn_{12}$. In this stage, many Ag atoms diffused into the solder, and the peritectic transformation might take place with a reaction of $L + AgZn \rightarrow L + AgZn + Ag_{59}Zn_{29}Sn_{12}$ rather than $L + AgZn \rightarrow L + AgZn + Ag_5Zn_8$ because the current Ag concentration is much higher than the highest Ag concentration (less than 3.0 wt.%) in Song's research,[22] as illustrated in Fig. 9. As shown in Fig. 3, there are two IMC layers in one particle. In fact, such a phenomenon was detected in every couple, as illustrated in Figs. 6b and 7b, c. With further increased aging time, for the Sn-4Ag-3Zn couple, the IMC was transformed into the Ag-Sn IMC. As shown in the ternary Sn-Ag-Zn phase diagram in Fig. 1,[43] the production of Ag_5Zn_8 has higher [Zn] and lower [Ag] than the production of $Ag_3Zn_{1-x}Sn_x$. In fact, [Ag] would increase with increasing aging time. Therefore, Ag-Zn IMC would be transformed into Ag-Sn-Zn IMC for the Sn-4Ag-3Zn/Ag joint. However, such a transformation was not detected for the Sn-4Ag-7Zn/Ag joint because Sn-4Ag-7Zn contains a higher concentration of Zn. At the same time, the thickness of the Ag-Zn IMC, close to the Ag substrates, exhibits no obvious changes for the Sn-4Ag-xZn/Ag joint. The reason may be that the equilibrium of Zn diffusion has been established. However, the transformations of the IMCs exhibit some differences between the liquid-state and solid-state reactions, especially for the Sn-4Ag-3Zn/Ag couple, because it is easier for Ag atoms to reach the IMCs than for Zn atoms to do so under solid-state conditions. As a result, the Zn-Ag IMC was transformed into Ag-Sn IMC under solid-state conditions.

Effects of Gravity and Surface Energy

For the Sn-4Ag-7Zn/Ag couple, the interfacial reaction was investigated on the lateral, top, and

bottom interfaces. As mentioned above, there are several differences among the three interfaces. It is inevitable to consider the effect of gravity. In fact, Tu et al.[44] considered the effect of gravity to explain the spalling phenomenon. Firstly, the densities of the molten Sn-4Ag and the Ag-Zn IMC particles are different. The theoretical densities of Ag_3Zn and AgZn are estimated to be 8.66 g/cm^3 and 8.26 g/cm^3, respectively, which are higher than that (7.17 g/cm^3) of Sn.[23] Therefore, it is possible that the Ag-Zn IMC particles on the top interface sedimented into the bottom interface in the static molten solder/Ag system because of the effect of gravity. Then the detachment of IMCs on the lateral interface would take place easily because of the effect of gravity. A similar sedimentation was also observed in Sn-Zn-Ag ternary solder.[23] Secondly, as shown in Fig. 10, the Ag_3Sn IMC did not detach from the lateral interface. However, the outer Ag-Zn IMC firstly becomes spherical particles and consequently detaches from the lateral interface, due to the weak adhesion between the Ag-Zn IMC and Ag_3Sn. Therefore, there are many Ag-Zn particles detached from the top interface so as to accumulate a number of spherical Ag-Zn particles on the bottom plate because of the weak adhesion. However, if the adhesion were very strong, IMC detachment may not happen during the reflow procedure.

CONCLUSIONS

The concentration of Zn in Sn-4Ag solder plays a crucial role in the composition of IMCs under solid- and liquid-state conditions. In the case of Sn-4Ag solder with low Zn addition (e.g., 1 wt.%), the Ag-Sn IMC is dominant at the interface except for a thinner Ag-Zn IMC. The AgZn IMCs were formed at the interface during the interfacial reaction with increasing concentration of Zn (e.g., 3 wt.% or 7 wt.%).

With increasing concentration of Zn in the Sn-4Ag solder, the IMC morphologies were transformed from continuous IMC layers into discontinuous and loose IMCs. Due to the weak adhesion between Ag-Zn and Ag-Sn IMCs in liquid Sn-4Ag-*x*Zn solders, discontinuous IMC layers were widely observed and often detected at the interface.

The growth kinetics of the IMC follows a parabolic law for the Sn-4Ag-1Zn/Ag couples, but it deviates from the parabolic law for the Sn-4Ag-3Zn/Ag couples because the IMC was detached from the interface and the thin Ag-Zn IMC retarded the growth of the IMC.

Experiments also revealed that the interfacial reactions on the top, bottom, and lateral positions in one sample have different features. Some spherical particles, which detached from the top position, accumulated on the bottom position; however, at the lateral position, the outer Ag-Zn IMC was detached from the Ag_3Sn IMC during the reflow procedure.

ACKNOWLEDGEMENTS

The authors would like to thank W. Gao, H.H. Su, Q.S. Zhu, J.T. Fan, X.H. An, and F. Yang for sample preparation, SEM observations, stimulating discussion, and corrections of the final manuscript. This work was financially supported by National Basic Research Program of China under Grant No. 2004CB619306 and the National Outstanding Young Scientist Foundation under Grant No. 50625103.

REFERENCES

1. M. Kerr and N. Chawla, *Acta Mater.* 52, 4527 (2004). doi:10.1016/j.actamat.2004.06.010.
2. M. Abtew and G. Selvaduray, *Mater. Sci. Eng. Rep.* 27, 95 (2000). doi:10.1016/S0927-796X(00)00010-3.
3. T.C. Chang, M.H. Hon, and M.C. Wang, *J. Alloy. Compd.* 352, 168 (2003). doi:10.1016/S0925-8388(02)01122-2.
4. J.M. Song, G.F. Lan, T.S. Lui, and L.H. Chen, *Scripta Mater.* 48, 1047 (2003). doi:10.1016/S1359-6462(02)00647-4.
5. J. Yu, D.K. Joo, and S.W. Shin, *Acta Mater.* 50, 4315 (2002). doi:10.1016/S1359-6454(02)00263-X.
6. C.E. Ho, Y.W. Lin, S.C. Yang, C.R. Kao, and D.S. Jiang, *J. Electron. Mater.* 35, 1017 (2006). doi:10.1007/BF02692562.
7. C.E. Ho, S.C. Yang, and C.R. Kao, *J. Mater. Sci. Mater. Electron.* 18, 155 (2007). doi:10.1007/s10854-006-9031-5.
8. D.J. Lee, D.H. Baek, K.K. Lee, K.M. Lee, and Y.J. Seo, *Z. Metallk.* 96 (2), 148 (2005).
9. J.M. Song, C.F. Huang, and H.Y. Chuang, *J. Electron. Mater.* 35, 2154 (2006). doi:10.1007/s11664-006-0326-3.
10. Y. Kariya and M. Otsuka, *J. Electron. Mater.* 27, 1229 (1998). doi:10.1007/s11664-998-0074-7.
11. S.K. Kang, D. Leonard, D.Y. Shih, L. Gignac, D.W. Henderson, S. Cho et al., *J. Electron. Mater.* 35, 479 (2006). doi:10.1007/BF02690535.
12. T. El-Ashram and R.M. Shalaby, *J. Electron. Mater.* 34, 212 (2005). doi:10.1007/s11664-005-0234-y.
13. F.J. Wang, F. Gao, X. Ma, and Y.Y. Qian, *J. Electron. Mater.* 35, 1818 (2006). doi:10.1007/s11664-006-0163-4.
14. S.C. Yang, C.E. Ho, C.W. Chang, and C.R. Kao, *J. Mater. Res.* 21, 2436 (2006). doi:10.1557/jmr.2006.0320.
15. Y.W. Yen, C.C. Jao, and C. Lee, *J. Mater. Res.* 21, 2986 (2006). doi:10.1557/jmr.2006.0369.
16. A. Fawzy, *Mater. Charact.* 58, 323 (2007). doi:10.1016/j.matchar.2006.05.013.
17. A. El-Daly and A.M. Addel-Daiem, *Phys. Status Solidi A* 198, 56 (2003). doi:10.1002/pssa.200306584.
18. F.J. Wang, X. Ma, and Y.Y. Qian, *Scripta Mater.* 53, 699 (2005). doi:10.1016/j.scriptamat.2005.05.013.
19. E. Saiz, C.W. Hwang, K. Suganuma, and A.P. Tomsia, *Acta Mater.* 51, 3185 (2003). doi:10.1016/S1359-6454(03)00140-X.
20. M.O. Alam and Y.C. Chan, *J. Appl. Phys.* 97, 7904 (2003). doi:10.1063/1.1628387.
21. G.P. Vassilev, S.K. Evtimova, J.-C. Tedenac, and E.S. Dobrev, *J. Alloy. Compd.* 334, 182 (2002). doi:10.1016/S0925-8388(01)01778-9.
22. J.M. Song and K.L. Lin, *J. Mater. Res.* 19, 2719 (2004). doi:10.1557/JMR.2004.0356.
23. J.M. Song and K.L. Lin, *J. Mater. Res.* 18, 2060 (2003). doi:10.1557/JMR.2003.0290.
24. M.D. Cheng, S.S. Wang, and T.H. Chuang, *J. Electron. Mater.* 31, 171 (2002). doi:10.1007/s11664-002-0202-8.
25. C.H. Wang and S.W. Chen, *Acta Mater.* 54, 247 (2006). doi:10.1016/j.actamat.2005.09.006.
26. T. Lauril, V. Vuorinen, and J.K. Kivilahti, *Mater. Sci. Eng. Rep.* 49, 1 (2005). doi:10.1016/j.mser.2005.03.001.
27. J.F. Li, S.H. Mannan, M.P. Clode, K. Chen, D.C. Whalley, C. Liu et al., *Acta Mater.* 55, 737 (2007). doi:10.1016/j.actamat.2006.09.003.

28. H.F. Hsu and S.W. Chen, *Acta Mater.* 52, 2541 (2004). doi:10.1016/j.actamat.2004.02.002.
29. C.M. Chen, K.J. Wang, and K.C. Chen, *J. Alloy. Compd.* 432, 122 (2007). doi:10.1016/j.jallcom.2006.05.116.
30. H.K. Kim and K.N. Tu, *Phys. Rev. B* 53, 16028 (1996). doi:10.1103/PhysRevB.53.16027.
31. G. Ghosh, *J. Electron. Mater.* 33, 1080 (2004). doi:10.1007/s11664-004-0108-8.
32. P.Y. Yeh, J.M. Song, and K.L. Lin, *J. Electron. Mater.* 35, 978 (2006). doi:10.1007/BF02692557.
33. S.C. Yang, C.E. Ho, C.W. Chang, and C.R. Kao, *J. Appl. Phys.* 101, 084911 (2007). doi:10.1063/1.2717564.
34. L. Muldawer, *J. Appl. Phys.* 22, 663 (1951). doi:10.1063/1.1700024.
35. R. Hultgren, P.D. Desai, D.T. Hawkins, M. Gleioser and K.K. Kelley, *Selected Values of Thermodynamic Properties of Binary Alloys* (Metals Park, OH: ASM International, 1973).
36. J.-W. Jang, L.N. Ramanathan, J.-K. Lin, and D.R. Frear, *J. Appl. Phys.* 95, 8286 (2004). doi:10.1063/1.1739530.
37. Y.-W. Yen and W.-K. Liou, *J. Mater. Res.* 22, 2663 (2007). doi:10.1557/jmr.2007.0339.
38. J.Y. Tsai, Y.C. Hu, C.M. Tsai, and C.R. Kao, *J. Electron. Mater.* 32, 1203 (2003). doi:10.1007/s11664-003-0012-7.
39. G.Z. Pan, A.A. Liu, H.K. Kim, K.N. Tu, and P.A. Totta, *Appl. Phys. Lett.* 71, 2946 (1997). doi:10.1063/1.120224.
40. A. Umantsev, *J. Appl. Phys.* 101, 024910 (2007). doi:10.1063/1.2424530.
41. Q.S. Zhu, Z.F. Zhang, J.K. Shang, and Z.G. Wang, *Mater. Sci. Eng. A* 435–436, 588 (2006). doi:10.1016/j.msea.2006.07.100.
42. Y.H. Xia, X.M. Xie, C.H. Lu, and J.L. Chang, *J. Alloy. Compd.* 417, 143 (2006). doi:10.1016/j.jallcom.2005.09.051.
43. G.P. Vassilev, E.S. Dobrev, S.K. Evtimova, and J.C. Tedenac, *J. Alloy. Compd.* 327, 285 (2001). doi:10.1016/S0925-8388(01)01562-6.
44. H.K. Kim, K.N. Tu, and P.A. Totta, *Appl. Phys. Lett.* 68, 2204 (1996). doi:10.1063/1.116013.